REMARKS

Claims 57-98 were pending in this application. In response to the Office Action dated July 11, 2004, claims 57-59 have been canceled and claims 61, 62, 63, 64, 66, 68, 70, 72, 73, 76, 77, 78, 79, 87, 88, 89, 90 and 95 have amended. New claims 99-104 have been added. Care has been exercised to avoid the introduction of new matter. Adequate descriptive support for the present Amendment should be apparent throughout the originally filed disclosure as, for example, the depicted embodiments and related discussion thereof in the written description of the specification, including page 11, lines 5-20. Applicants submit that the present Amendment does not generate any new matter issue. Entry of the present Amendment is respectfully solicited. It is believed that this response places this case in condition for allowance. Hence, prompt favorable reconsideration of this case is solicited.

Initially Applicants note that a response to the Examiner's IDS requirement was submitted on August 8, 2005, within the one-month reply period set by the Examiner. A legible copy of the reference was resubmitted for the Examiner's consideration. Accordingly, Applicants submit that the IDS filed in September 3, 2004 fully complies with 37 C.F.R. 1.98.

Claims 62, 68 and 95 have been amended to address the minor informalities identified by the Examiner. Accordingly, reconsideration and withdrawal of the objection are solicited. Claim 76 has been amended to depend solely from claim 75, thereby addressing the multiple dependency objection. Accordingly, reconsideration and withdrawal of the objection to claims 76-77 and are solicited.

Claims 60-63, 65, 66, 67, 68, 69, 74, 75, 82-86 and 93-98 were rejected under the first paragraph of 35 U.S.C. § 112 as allegedly failing to comply with the written description requirement. Applicants traverse.

The resin coating in Table 5 is formed by injection molding. It is common knowledge for persons skilled in the art that a resin optical component made by injection molding has a mirror-finished surface. Contrary to the Examiner's assertion, it is possible to compare Table 4 with Table 5. In the rejection, the Examiner conducted multiplication of Ti/Tv of the resin part and the Ti/Tv of the ceramic in Table 2 without correcting the thickness of the resin in Table 4. Thus, the apparent products, Ti/Tv (ceramic part) × Ti/Tv (resin part), for Sample No. 3 and Sample No. 6 became greater than Ti/Tv (lens) in Table 5. By correcting the thickness of the resin in Table 4 from 0.1 mmt to 0.05 mmt, multiplication of Ti/Tv of the resin part and the Ti/Tv of the ceramic in Table 2 gives a value smaller than Ti/Tv (lens) in Table 5 in both Samples No. 3 and No. 6.

With respect to Claim 60, whereas Sample No. 3 in Table 5 provides values for Ti/Tv (lens) of a resin layer coated on the ceramic part, Table 4 provides Ti/Tv (resin part) for resin samples with mirror-finished surfaces. Although line 13 in page 35 of the subject application describes "mirror finished surfaces", only the ceramic part requires mirror finishing. In general, it is understood in the art that finishing is not needed for resins. As an example, the Examiner's attention is directed to Japanese Unexamined Utility Model Registration Application Publication No. 62-79119 describes at lines 12 to 17 of page 3 of the English translation (**Appendix A**), that an optical component made by injection molding of polyethylene has mirror-finished surfaces. Moreover, Sherber (U.S. Pat. No. 4,708,419), previously cited by the Examiner in the December 21, 2004 Office action, describes at col. 2, line 25 and lines 64-66 that "[t]he smooth surface of

thermoplastic material (including polyethylene) does not require any specific surface finishing such as polishing or grinding." In view of the above, it is understood in the art that optical components produced by a technique, such as injection molding for providing resin coating, have mirror-finished surfaces. Since similar mirror surfaces are produced in the present application, it is possible to compare the aforementioned values.

With respect to claim 62, the thickness in Sample 3 and Sample 6 of Table 5 is 50 μm, whereas the thickness of resin samples No. 1 and No. 2 in Table 4 is 100 μm. Thus, the thicknesses cannot be directly compared. For example, Sample No. 4 of Table 5 in which the thickness of coated resin layer is 100 μm provides a Ti/Tv (lens) of 5015, which is greater than the product 3487 given by [a Ti/Tv (ceramic part) of 3170 in Table 2] × [a Ti/Tv (resin part) of 1.1 in table 4], thereby supporting the subject matter recited in claim 62.

Furthermore, by thickness correction, all samples including Samples No. 3 and 6 satisfy the relationship Ti/Tv(lens) > Ti/Tv (ceramic part) × Ti/Tv (resin part).

The process of the above described calculation is based on the description in lines 6 to 10, right column, p. 77 of the attached document (**Appendix B**), "SEI Technical Review No. 54, June 2002, Optical Characteristics of an Infrared Translucent Close-Packed ZnS Sintered Body" stating that "the transmittance of infrared optical ceramics is given by the Lambert-Beer Equation, and if the material (i.e., refractive index) and thickness are specified, then the transmittance (Ti or Tv) is determined by the absorption coefficient". The specific process is described below for the Examiner's consideration.

Correction Calculation

(i) Ti, Tv, the thickness (100 μm), and a typical refractive index of polyethylene at each wavelength (n = 1.6 for Ti at a wavelength of 10 μm, and n = 1.5 for Tv at a wavelength of

830 nm) set forth Table 4 were substituted into Equation (2) and Equation (11) to give the absorption coefficients βi and βv. Note that although Equation (11) is applied to Ti in the infrared range, the equation is also applicable to Tv in the visible range.

Example: Sample No. 1 in Table 4

Ti = 81%, Thickness (t) = 0.1 mm, Refractive index ni = 1.6 → βi = 1.013

Tv = 74%, Thickness (t) = 0.1 mm, Refractive index nv = 1.5 → βv = 2.195

(wherein n_m in Equation (2) in the infrared range is represented by ni and that in the visible range is represented by nv; and β is given by Equation (10))

(ii) Based on the absorption coefficients β obtained as above, the refractive indexes n, and a predetermined thickness t (e.g., 0.05 mm), transmittances Ti and Tv are calculated by Equation (11) to give Ti/Tv (resin).

Example: Sample No. 1 in Table 4

·βi = 1.013, Refractive index ni = 1.6, Thickness = 0.05 mm → Ti = 85.2%

·βv = 2.195, Refractive index nv = 1.5, Thickness = 0.05 mm → Tv = 82.6%

→ Ti/Tv(resin) = 1.03

(iii) Ti/Tv (lens) in Table 5 and Ti/Tv (ceramic part) in Table 2 × Ti/Tv (resin) calculated as above are compared.

Example: The lens in Table 5, the ceramic raw material in Table 2, and the resin in the calculation above are compared:

·Ti/Tv (lens) = 4474 for Sample No. 3 in Table 5

·Ti/Tv (ceramic) = 3170 for Sample No. 2 in Table 2

Ti/Tv (resin) = 1.03 according to the above-described calculation

→ Ti/Tv (ceramic) × Ti/Tv (resin) = 3271

Thus, Ti/Tv (lens) $\geq$ Ti/Tv (ceramic) $\times$ Ti/Tv (resin).

The results of calculations for other samples are shown in the attached Table (**Appendix C**).

Applicants, therefore, submit that in view of the foregoing, one having ordinary skill in the art would have no difficulty understanding the subject matter of claims 60-63, 65, 66, 67, 68, 69, 74, 75, 82-86 and 93-98, particularly when reasonably interpreted in light of the written description of the specification. The present disclosure conveys with reasonable clarity to those skilled in the art that the inventors were in possession of the invention. In other words, one skilled in the art, reading the original disclosure, would reasonably discern the limitation at issue in the claims. *Waldemar Link GmbH & Co. v. Osteonics Corp.*, 32 F.3d 556, 558, 31 UPSQ2d 1855, 1857 (Fed. Cir. 1994). Thus, the imposed rejection under the first paragraph of 35 U.S.C. § 112 has been overcome and, hence, Applicants respectfully solicit withdrawal thereof.

Claims 57-59, 64, 78 and 87-90 were rejected under 35 U.S.C. § 103(a) as being unpatentable over Tower et al. (U.S. Pat. No. 6,020,628, hereinafter "Tower") in view of Grossinger et al. (U.S. Pat. No. 5,712,622, hereinafter "Grossinger") Silvestrini et al. (U.S. Pat. No. 4,323,619, hereinafter "Silvestrini") and Raj et al. (U.S. Pat. No. 5,183,602, hereinafter "Raj").

Claims 66, 67, 91 and 92 were rejected under 35 U.S.C. § 103(a) as being unpatentable over Tower in view of Grossinger, Silvestrini and Raj and further in view of Carnall, Jr. et al. (U.S. Pat. No. 3,131,238, hereinafter "Carnall").

Claims 68, 69, 91 and 92 were rejected under 35 U.S.C. § 103(a) as being unpatentable over Tower in view of Grossinger, Silvestrini and Raj and further in view of Roy et al. (U.S. Pat. No. 3,974,249, hereinafter "Roy").

Claims 57-59, 64, 70, 71 and 87-90 were rejected under 35 U.S.C. § 103(a) as being unpatentable over Castleman (U.S. Pat. No. 6,153,881, hereinafter "Castleman") in view of Grossinger, Silvestrini and Raj.

Claims 72 and 73 were rejected under 35 U.S.C. § 103(a) as being unpatentable over Castleman in view of Grossinger, Silvestrini and Raj and further in view of Erismann (U.S. Pat. No. 5,818,337).

Claims 79 and 80 were rejected under 35 U.S.C. § 103(a) as being unpatentable over Castleman in view of Grossinger, Silvestrini and Raj and in further in view of Adachi et al. (U.S. Pat. No. 4,302,674, hereinafter "Adachi").

Claims 81 was rejected under 35 U.S.C. § 103(a) as being unpatentable over Castleman in view of Grossinger, Silvestrini, Raj and Adachi and further in view of Erismann.

Applicants respectfully traverse each of the rejections under 35 U.S.C. § 103(a) identified above for the reasons set forth *infra*. Claims 57-59 have been canceled and, therefore, the above rejections under 35 U.S.C. § 103(a) are moot. Moreover, new independent claims 99-102 have been added and Applicants submit that new claims 99-104 are free from the applied art. Applicants submit that none of the applied references, alone or in combination, teaches or remotely suggests the present claimed subject matter.

Tower discloses a sensor comprising a ceramic lens, a supporting part, and a detection part. Grossinger discloses an optical element in which visible light is shielded by pigment particles and Silverstrini discloses a dispersion of a pigment. Applicants submit that Tower fails to disclose a ceramic lens containing any pigment. With Grossinger and Silverstrini, the base ingredient is a resin, such as polyethylene, however, neither discloses a ceramic containing the specific pigments. Moreover, Raj is limited to diamond particles dispersed in ceramics and fails

to disclose the dispersion of diamond pigment in a range of 0.001 mass% to 1 mass%. None of the references alone or in combination teaches ceramic containing the specific pigments as disclosed in new claim 99 or the specific carbon black and diamond in the required amounts of claims 100 and 101.

Independent claim 99 describes a ceramic infrared sensor, having a lens body, comprising ceramic, a supporting part, which supports the lens body, and a detection part, which detects the light that has been transmitted through the lens body. A pigment that shields visible light is contained in the lens body and the pigment is selected from graphite, titanium black, an iron oxide, molybdenum, tungsten, iron, nickel, cobalt, copper, silver, compounds thereof, TiO_2, BN, AlN, ZnO, ZnS, or mixtures thereof.

Independent claim 100 describes a ceramic infrared sensor, having a lens body, comprising ceramic, a supporting part, which supports the lens body, and a detection part, which detects the light that has been transmitted through the lens body. The pigment is carbon black in a range of 0.001 mass% to 0.01 mass%, graphite, titanium black, an iron oxide, molybdenum, tungsten, iron, nickel, cobalt, copper, silver, compounds thereof, TiO_2, BN, AlN, ZnO, ZnS, or mixtures thereof.

Independent claim 101 describes a ceramic infrared sensor, having a lens body, comprising ceramic, a supporting part, which supports the lens body, and a detection part, which detects the light that has been transmitted through the lens body. The pigment is diamond in a range of 0.001 mass% to 1 mass%, graphite, titanium black, an iron oxide, molybdenum, tungsten, iron, nickel, cobalt, copper, silver, compounds thereof, TiO_2, BN, AlN, ZnO, ZnS, or mixtures thereof.

Independent claim 102 describes a ceramic infrared sensor, having a lens body, comprising ceramic, a supporting part, which supports the lens body, and a detection part, which detects the light that has been transmitted through the lens body. The pigment is carbon black in a range of 0.001 mass% to 0.01 mass%, diamond in a range of 0.001 mass% to 1 mass%, graphite, titanium black, an iron oxide, molybdenum, tungsten, iron, nickel, cobalt, copper, silver, compounds thereof, TiO_2, BN, AlN, ZnO, ZnS, or mixtures thereof.

Accordingly, the proposed combination of references would not yield the claimed inventions since none of the references discloses a ceramic containing the specific pigments as disclosed in new claims 99-102, much less the specific amount of carbon black and diamond required in claims 100, 101 and 102. *Uniroyal, Inc. v. Rudkin-Wiley Corp.*, 837 F.2d 1044, 5 USPQ2d 1434 (Fed. Cir. 1988). The only motivation for such a limitation is Applicants' own disclosure. Applicants' disclosure, however, is forbidden territory for the Examiner to obtain the requisite motivation for combining the applied prior art. *Panduit Corp. v. Dennison Mfg. Co.*, 774 F.2d 1082, 227 USPQ 337 (Fed. Cir. 1985).

Although the Examiner asserts that one of ordinary skill in the art would have applied the techniques set forth in Grossinger, Silverstrini and Raj to the technique set forth in Tower, Applicants maintain that unlike resins, ceramics rarely allow perfect dispersion of minute amounts of additives. Thus, a person skilled in the art would not have been easily successful in attempting such a technique. In fact, the Examiner's attention is directed to Example 1 of the present specification, wherein special techniques are necessary in order to disperse pigment particles in ceramics. It is well established that the requisite motivation to support an ultimate legal conclusion of obviousness under 35 U.S.C. § 103 is not an abstract concept, but must stem from the applied prior art as a whole and have realistically impelled one having ordinary skill in

the art to modify a reference or combine references to arrive at the claimed invention. *In re Deuel*, 51 F.3d 1552, 34 USPQ2d 1210 (Fed. Cir. 1995); *In re Newell*, 891 F.2d 899, 13 USPQ2d 1248 (Fed. Cir. 1989). Further, it is well settled that the recognition of the source of a problem constitutes evidence of nonobviousness. *In re Sponnoble*, 405 F.2d 578, 160 USPQ 237 (CCPA 1969). Thus, Applicants submit that one having ordinary skill in the art would not have been realistically impelled to modify Tower's sensor with Grossinger, Silverstrini and Raj to arrive at the claimed inventions.

It is believed that all pending claims are now in condition for allowance. Applicants therefore respectfully request an early and favorable reconsideration and allowance of this application. If there are any outstanding issues which might be resolved by an interview or an Examiner's amendment, the Examiner is invited to call Applicants' representative at the telephone number shown below.

To the extent necessary, a petition for an extension of time under 37 C.F.R. 1.136 is hereby made. Please charge any shortage in fees due in connection with the filing of this paper, including extension of time fees, to Deposit Account 500417 and please credit any excess fees to such deposit account.

Respectfully submitted,

McDERMOTT WILL & EMERY LLP

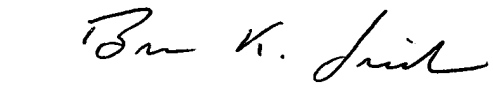

Brian K. Seidleck
Registration No. 51,321

Please recognize our Customer No. 20277 as our correspondence address.

600 13th Street, N.W.
Washington, DC 20005-3096
Phone: 202.756.8000 BKS:idw
Facsimile: 202.756.8087
Date: **December 8, 2005**

Utility Model Application

Publication number: Jitsukaishou 62-79119

Date of publication of applicaion : May 20, 1987

SPECIFICATION

1. Title of the Device: PACKAGE FOR OPTICAL SENSOR

2. Claim for Utility Model Registration

(1) A package for an optical sensor, the package being composed of a synthetic resin and attachable to a substrate having an optical sensor element, characterized in that a light transmission window is integrally formed with the package.

3. Detailed Description of the Device

(Industrial Field of Application)

The present device relates to a structure of a package, which is a component of an optical sensor, such as an infrared sensor or a ultraviolet sensor.

(Related Art and Problems)

A typical optical sensor is produced by attaching a package 3' composed of a synthetic resin or a metal, such as a 42 alloy, onto a substrate 2' having an optical sensor element 1', as shown in Fig. 3.

An infrared sensor is described here as an example. An opening 4' formed in a top surface of the package is provided with a multilayer film infrared interference filter 5' when selective transmission of infrared rays in a particular wavelength range is required, or with a polyethylene film bonded

thereto when selective transmission of only infrared rays is not required in actual use. In the latter case, the film only has functions of isolating the infrared sensor element from the external environment and protecting the element from the physical external force.

In any case, a filter or a polyethylene film is bonded onto the opening in the package; thus, the assembly of the sensor requires a troublesome, complicated process. Moreover, since the opening is sealed by attaching a thin filter or film, external air may enter or breakage may occur due to external force when the filter or film is deteriorated during the use.

(Means for Solving the Problem)

This device is applied to an optical sensor that does not require selective transmission of light in a particular wavelength range, the device having a light-transmission window integrally formed with a synthetic resin package attachable to the substrate having the optical sensor element.

(Operation)

Since the light-transmission window is integrally formed with the package, the strength of the light-transmission window is increased, and the function of isolating the optical sensor from the external environment and the resistance to the physical external force can be enhanced. Moreover, assembly of the optical sensor is facilitated.

(Example)

Figs. 1 and 2 show examples used for infrared sensors that do not require selective transmission of only the infrared rays.

Reference numeral 1 denotes a box-shaped package composed of polyethylene. At the center of the top surface, a light-transmission window 2

having a thickness of 0.2 mm or less is integrally formed with the package by injection molding. Here, when the thickness of the light-transmission window 2 is 0.2 mm or more, the attenuation of the transmitted light becomes large, which is not practical. Naturally, both the upper and lower surfaces of the light-transmission window are mirror-finished.

The inner surface of the package 1 has opposing projections 3. In the course of assembly of the infrared sensor, the package can be easily attached to the substrate by inserting these projections to recesses 6 corresponding to the projections 3, the recesses being formed in the outer surface of the substrate 5 having the infrared sensor element 4.

According to the shape of the substrate, the shape of the package can be adjusted to a desired shape, such as a cylindrical shape. Moreover, it is possible to attach a filter that can selectively transmit light in a particular wavelength range onto the light transmission window.

(Advantages)

Since the package and the light-transmission window are integrally formed, the optical sensor has a large strength and is highly resistant to deterioration, the assembly is easy, and the cost can be reduced.

4. Brief Description of the Drawings

Fig. 1 is a cross-sectional view and Fig. 2 is a perspective view of a package and a substrate. Fig. 3 is a cross-sectional view of a conventional package.

1: package 2: light transmission window

5: substrate

第1図 Fig. 1

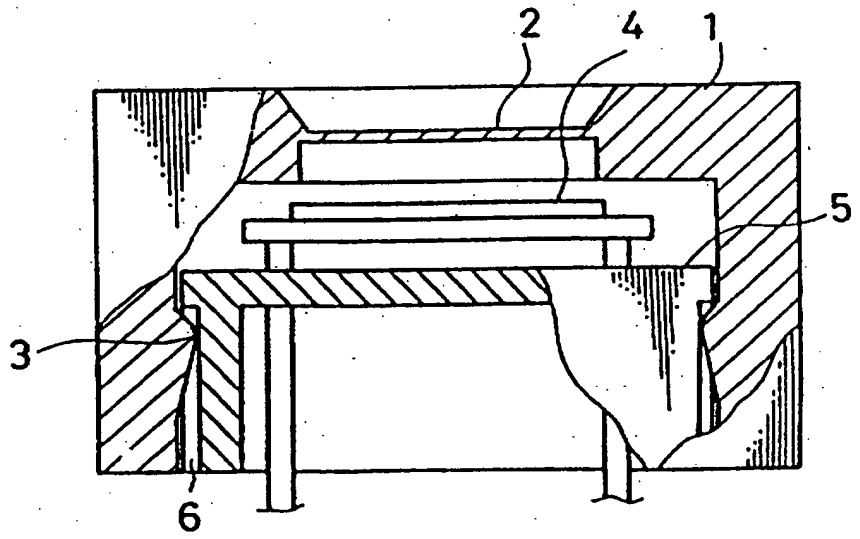

第2図 Fig. 2

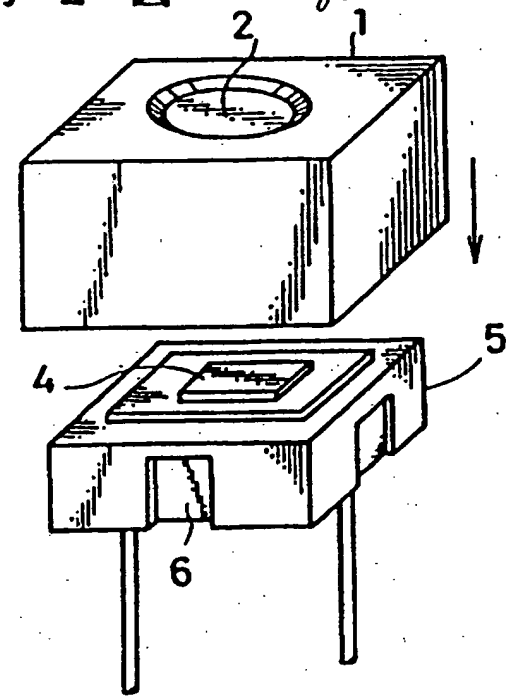

第3図 Fig. 3

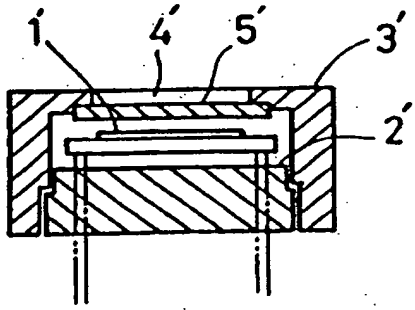

代理人弁理士 山上正晴
実開62-79119

SET

Optical Characteristics of an Infrared Translucent Close-Packed ZnS Sintered Body

Masato HASEGAWA, Osamu KOMURA, Akira YAMAKAWA,
Kenichiro SHIBATA, Hajime NAITO,
Shigeru NAKAYAMA and Akihito FUJII

SUMITOMO ELECTRIC

Optical Characteristics of an Infrared Translucent Close-Packed ZnS Sintered Body

Masato HASEGAWA, Osamu KOMURA, Akira YAMAKAWA, Kenichiro SHIBATA, Hajime NAITO, Shigeru NAKAYAMA and Akihito FUJII

1. Introduction

Sensor technology employing infrared rays is in wide use today, mainly for amenity, convenience and safety. Applications are far ranging: in industrial fields such as online monitoring of plants and manufacturing lines; in crime and accident prevention fields such as round-the-clock intruder and fire monitoring; in temperature measurement for microwave ovens; in household appliance fields such as ear thermometers and air conditioners; and in the automotive field for night vision. The importance of this technology has grown steadily in recent years.

Equipment such as that mentioned above employs infrared radiation at a variety of wavelengths. There are types designed that use 3 to 5 μm for detecting comparatively high temperatures (as for fire detection), types that use 8 to 12 μm (corresponding to the temperature of the human body), and even types that can detect both wavelength bands. For the optical components that comprise the windows and lenses of these sensors, there is an increasing need to lower costs and increase practical performance(e.g., the ability to transmit light across a wide wavelength band, or to block light of a specific wavelength band). Of these devices, infrared image sensors for the 8 to 12 μm band are expected to become more important in applications involving detection of the human body.

The spectral characteristics of typical infrared optical materials used for the 8 to 12 μm wavelength band are shown in **Figure 1**, and the basic characteristics are listed in **Table 1.**[1)]

ZnS, ZnSe and Ge are already in practical use for manufacturing devices using processes such as the chemical vapor deposition (CVD) method and melting/solidification. Although these materials exhibit outstanding optical characteristics, constraints of cost, size, and shape have limited them to use in high-cost products requiring high functionality, such as those for thermography.

Conversely, polyolefine-based organic materials such as polyethylene (PE) have been widely used for low-cost window materials and lenses. However, organic materials have multiple infrared absorption peaks near

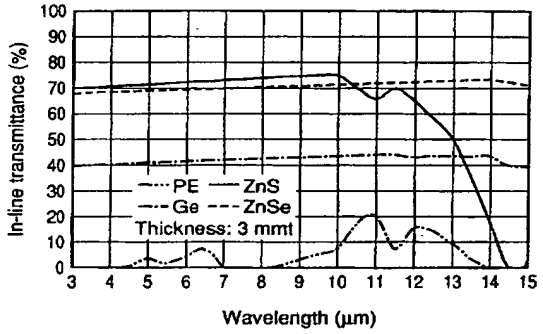

Fig. 1. Spectral caracteristics of infrared optical materials

Table 1. Characteristics of typical infrared optical materials for 8 ~ 12μm wave length band

Term	Unit	ZnS (CVD)	ZnSe (CVD)	Ge	PE
Crystal class		Cubic	Cubic	Cubic	–
Melting point	K	2103	1793	1210	407
Density	$\times 10^3 kg/m^3$	4.08	5.27	5.35	0.96
Refractive index at 10 μm		2.20	2.41	4.01	1.58
Young's modulus	GPa	75	70	103	–
Flexural strength	MPa	98	55	100	34
Knoop hardness number		230	105	800	–
Thermal conductivity	W/(m · K)	17	18	31	–
Thermal expansion coefficient	$\times 10^{-6}/K$	6.7	7.1	6.1	80

Photo 1.

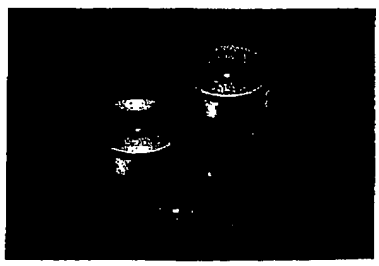

Photo 2.

the 10 μm wavelength, so translucence is less than satisfactory, and these materials are not used for highly sensitive infrared sensors.

In order to meet the need for low-cost optical materials with high functionality, the authors have developed an infrared translucent close-packed ZnS sintered body (hereafter referred to as a "ZnS sintered body") using a powder sintering method with outstanding potential for mass production.

With heat-type infrared sensors, it is essential to cut noise light in the visible to near/mid infrared range. By exploiting the advantages of the powder method and adding specific elements, the authors have also developed a ZnS sintered body that functions as an optic filter for cutting such noise light. Examples of these products are shown in **Photos 1 and 2.**

Using the powder sintering method, the authors developed several infrared optical ceramics. Practical use of magnesium fluoride (MgF_2)[2] and spinel ($MgAl_2O_4$)[3] as an optical material for infrared sensors in the 3 to 5 μm wavelength band was achieved, as was use of barium fluoride (BaF_2)[4] for use in the 8 to 12 μm wavelength band. Since these are all polycrystals, no cleavage was encountered (as is inherent with monocrystals), and they are distinctive in having outstanding mechanical strength and workability.

2. Manufacturing Process for a ZnS Sintered Body

2-1 Manufacturing Method

The key points in the development of infrared optic ceramics using powder sintering technology are: control of impurities and second-phase precipitation, which cause light scattering and thereby reduce the transmittance; and minimizing of residual pores in the process of sintered close packing. To address these points we used high-purity materials and a high-purity process to adequately eliminate pores, and used the hot press method to obtain translucence by close-packing at almost 100% of the theoretical density. The manufacturing process is shown in **Figure 2.**

The principles underlying the hot press method are shown in **Figure 3.** The mold is filled with powder material, and enhanced sintering is performed by pressurizing at high temperature under a vacuum, forcing pores out to obtain a microuniform sintered body with controlled crystal grain formation.

During the procedure the purity, particle diameter, form and other properties of the ZnS raw material powder are carefully controlled, and hot press conditions such as atmosphere, temperature, pressure and time are optimized.

The raw material powders that are used have average particle diameters of 1.5 μm or less, and any infiltration of suspended particles in the air into the powder would cause inclusions in the polycrystal, so the powder is handled in a clean room. The obtained sintered body has a relative density (relative to the theoretical density) of 99.9%, and is comprised of a microstructure with an average particle diameter of 3.3 μm. The crystal structure is shown in **Figure 4.**

A sintered body obtained using the method described above was machined and polished into the necessary shape, and its properties evaluated. In-line transmittance was measured by fabricating a 20-mm diameter disk sample with adjusted thickness. In the infrared range at and above the wavelength of 2.5 μm, a Fourier transform type infrared spectrophotometer (FT-IR) from JASCO Corporation was used. An ultraviolet/visible spectrophotometer (UVS) from Hitachi, Ltd. was used in the wavelength range 0.4 to 2.6 μm. For high temperature measurement in the infrared range, a small heater was installed in the FT-IR sample

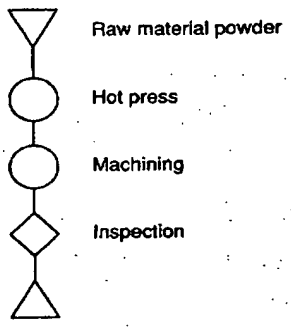

Fig. 2. Manufacturing process for a ZnS sintered body

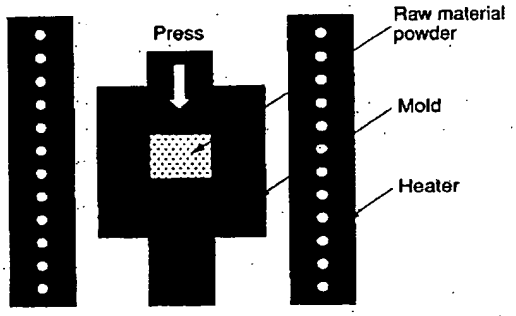

Fig. 3. Hot press manufacturing method

Fig. 4. Micro structure of a ZnS sineered body

chamber, and measurement was performed in the temperature range of room temperature (RT) to 500°C. Bending strength was measured using an all-purpose mechanical tester from Instron Corporation. The 4-point bending method conforming to JISR1601 was used as the measurement method, and the test piece shape was set at 3 × 4 × 40 mm. Measurement at high temperature was performed in the temperature range RT to 500°C based on JISR1604. Young's modulus was measured using the ultrasonic pulse method conforming to JISR1602. Knoop hardness was measured with a load of 15 g × 10 sec using a microhardness tester. Thermal conductivity was measured with a ø10 × 3 mm sample using the laser flash method, based on JISR1611. The refractive index was found by measuring reflectance with an FT-IR and then using the Kramers-Kronig conversion. **Figure 5** shows the results of measuring transmittance to infrared rays. In the sensitive wavelength band for detecting the human body of 8 to 12 μm, the material exhibited translucence performance equivalent to CVD-ZnS, but transmittance dropped on the short wavelength side (wavelength 3 to 5 μm band).

2-2 Quantitative Analysis Using a Light Scattering Model

The drop in transmittance of the polycrystal translucent ceramic on the short wavelength side is due to various scattering factors inside the sintered body, as shown in **Figure 6**. It may be expressed using the Lambert-Beer Equation (1).[5]

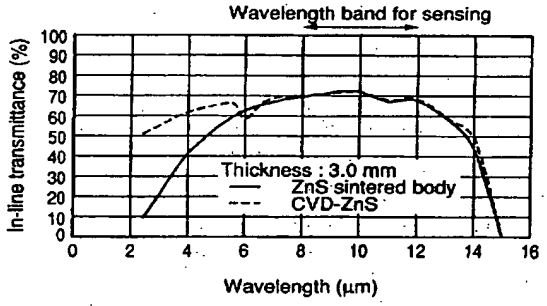

Fig 5. Spectral caracteristics of a ZnS sintered body and CVD-ZnS

$$T = (1 - R)^2 \cdot \exp(-\beta t) \quad \cdots\cdots (1)$$

$$R = (n_m - 1)^2 / (n_m + 1)^2 \quad \cdots\cdots (2)$$

Where:

R : Reflectance
nm : Refractive index of ZnS which is the matrix
β : Absorption coefficient
t : Material thickness

$$\beta = \alpha_0 + S_{pore} + S_{de} + S_{OP} \quad \cdots\cdots (3)$$

Where:

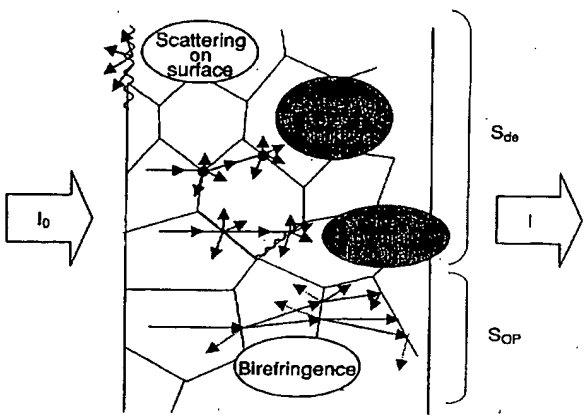

Fig 6. Light scatiering factors for transparent ceramics

α_0 : Material specific absorption (Multi-phonon mode; electron transition between band gaps)
S_{pore} : Light scattering due to residual pores
S_{de} : Scattering and absorption due to impurities and 2nd phase precipitation
S_{OP} : Scattering due to optical anisotropy at crystal grain boundary

In this instance high-purity raw materials and processes were used, so the effect of scattering attributable to impurities and the second-phase precipitation is thought to be small. Since ZnS has no optical anisotropy, S_{OP} can also be ignored. Thus, scattering due to residual pores is regarded as the primary cause, and we attempted to quantitatively analyze the cause of the drop in transmittance using light scattering theory.

The amount of light scattering due to pores existing in the sintered body is calculated by adopting the scattering model shown in **Figure 7**. In this model, it is assumed that pores are perfectly spherical and evenly dispersed in the sintered body. As such, S_{pore} is given by Equation (4).

$$S_{pore} = N_0 \cdot C_{sca} \quad \cdots\cdots (4)$$

Where:

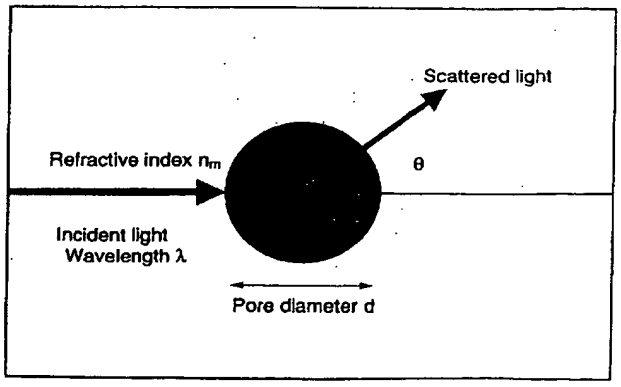

Fig 7. Model of light scattering

N_0 : Pore density (Number of pores per unit volume)
C_{sca}: Scattering cross-section area due to unit grain

If we assume (to simplify the model) that pore diameters are of a monodispersion with no distribution, then:

$$N_0 = \frac{V}{\frac{4}{3}\pi\left(\frac{d}{2}\right)^3} \quad \cdots\cdots (5)$$

Where:
V : Porosity
d : Pore diameter

If the scattering cross-section area C_{sca} is replaced with a dimensionless scattering efficiency coefficient Q_{sca} ($= C_{sca}/\pi(d/2)^2$), then from Equations (4) and (5):

$$S_{pore} = \frac{3VQ_{sca}}{4\left(\frac{d}{2}\right)} \quad \cdots\cdots (6)$$

Here, when the grain diameter of the light scattering body reaches the order of the light wavelength, Mie scattering begins to dominate,[5] so Q_{sca} is handled assuming this to be dominant.

The strict solution for Mie scattering is found by applying Maxwell's electromagnetic equations to spherical grains as the scattered light intensity distribution for the vertical and horizontal defection component for the scattered light intensity of one scattering body. This indicates that it is a function of the scattering angle, grain diameter parameter X and relative refractive index M.

The scattering cross-section area C_{sca} is found by integrating the scattering light distribution over the entire space,[6],[7] and under conditions where the refractive indices of the spherical grain and matrix are close, and there is no light absorption by spherical particles. An approximate solution may be calculated from the following equation.[6]

$$Q_{sca} = 2 - \frac{4}{\rho}\sin\rho + \frac{4}{\rho^2}(1 - \cos\rho) \quad \cdots\cdots (7)$$

$\rho = 2X(M - 1)$
$X = 2\pi(d/2)/\lambda$
$M = n_0/n_m$

Where:
λ : Wavelength of applicable infrared light

To conduct simulation using the above formula, we used a value from literature[1] for the necessary parameter α_0, and an actual measured value for the refractive index n_m. William et al. determined that with regards to the pore diameter d, the values observed with a scanning electron microscope (SEM) correspond well with the simulation values using Mie scattering.[8] So we measured the diameter of 100 pores via SEM structure observation, and obtained an average pore diameter of d = 0.4 μm. **Figure 8** shows an example of residual pore diameter determined by SEM structure observation. The results of calculating in-line transmittance using this method matched well with actual measurements, as indicated in **Figure 9**.

We determined using the above methods that the in-line transmittance of the ZnS sintered body is affected by scattering due to residual pores. Using calculations we consequently investigated the pore diameter dependence of transmittance, and found the residual pore diameter necessary to obtain transmittance on a par with CVD-ZnS.

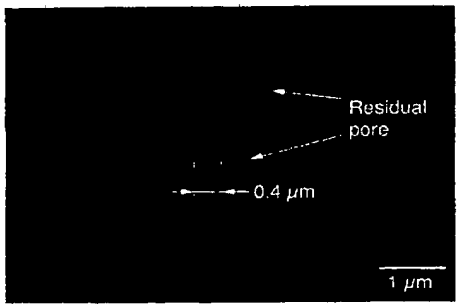

Fig. 8. Residual pores of a ZnS sintered body

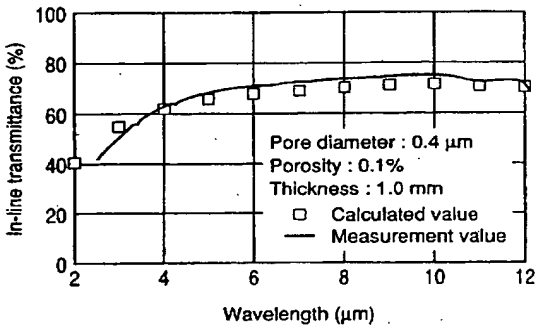

Fig. 9. Comparison between values calculated from Mie scattering theory and measured values for a ZnS sintered body

As shown in **Figure 10**, pore diameter has almost no

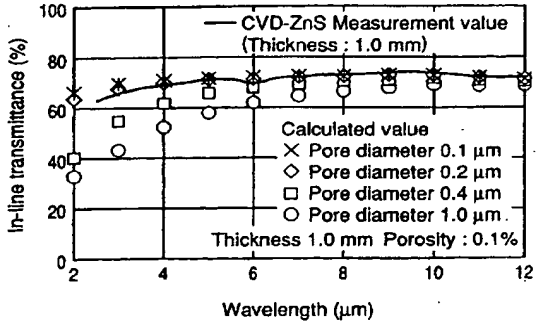

Fig. 10. Comparison between calculated transmittance values for a ZnS sintered body and measured values for CVD-ZnS (effects of pore diameter)

effect in the wavelength range 8 to 12 μm, but in the short wavelength range of 8 μm or less, transmittance improves as pores become smaller. We determined that the pore diameter must be set to 0.2 μm or less in order to obtain translucence characteristics equivalent to CVD-ZnS.

2-3 Study of a ZnS Sintered body

We investigated the effects on control of pore diameter of optimizing sintering conditions.

As a result, we obtained a sintered body with a relative density of 99.9%, an average pore diameter of 0.2 μm and a crystal grain diameter of 1.7 μm, as shown in **Figs. 11 and 12**. A comparison is shown in **Fig. 13** of the results for this ZnS sintered body, those for a sintered body with a average pore diameter of 0.4 μm, the infrared transmittance measurement results for CVD-ZnS, and calculation results using the simulation.

Fig. 11. Microstructure of a pore-controlled ZnS sintered body

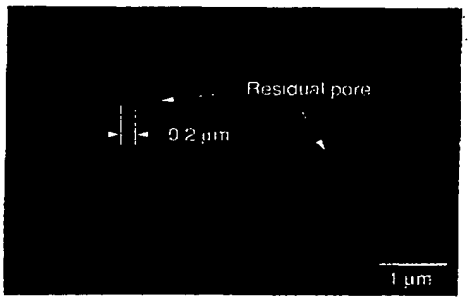

Fig. 12. Controlled residual pore of a ZnS sintered body

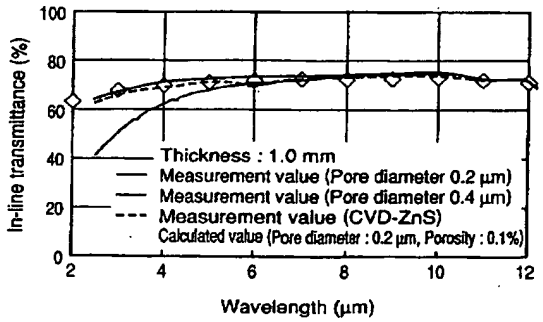

Fig. 13. Transmittance of CVD-ZnS and ZnS sintered bodies (calculated and measured values)

We confirmed that there is a good match between measured and calculated values, that translucence characteristics in the short wavelength range are improved, and that it is possible to obtain a ZnS sintered body with translucence characteristics equivalent to those of CVD-ZnS.

3. ZnS Sintered Body Characteristics

3-1 General Characteristics

Figure 14 shows infrared spectral characteristics in the wavelength range 2 to 15 μm for each thickness of the ZnS sintered body produced. It can be seen that all have good translucence characteristics in the sensor sensitivity wavelength range of 8 to 12 μm. Near 11 and 12 μm where ZnS has a distinctive absorption peak, the graph shows a tendency for transmittance to drop as thickness increases, but it is evident that the overall drop is comparatively small, and the contribution of absorption/scattering is low.

Figure 15 shows infrared spectral characteristics for a 4-mm thick ZnS sintered body with an anti-reflective (AR) coating, a technique typically used for improving practical translucence. Compared to the results with no coating, surface reflection loss is suppressed, and we confirmed that at a wavelength of 10 μm, transmittance is improved by approximately 10% with a single-sided

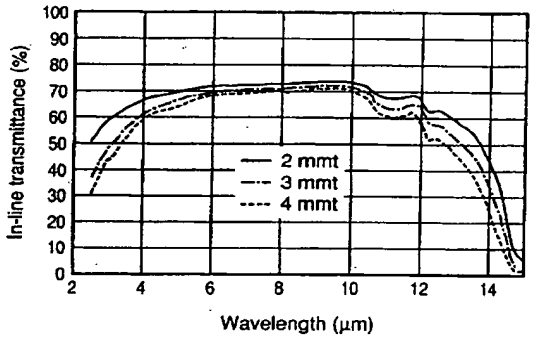

Fig. 14. Typical spectral caracteristics of ZnS sintered bodies

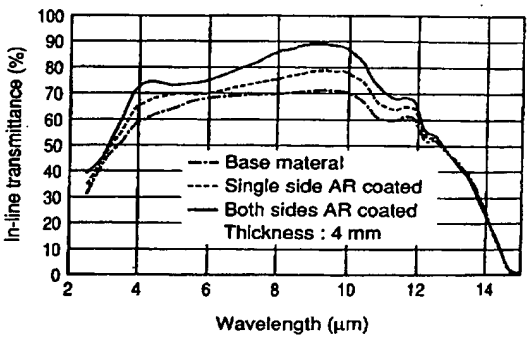

Fig. 15. Spectral characteristics of ZnS sintered bodies: and uncoated; AR coated on single side; AR coated on both sides

coating and by approximately 20% with a double-sided coating.

Figure 16 shows the results of measuring the refractive index at room temperature (24°C) with wavelengths between 2.5 and 15 μm. The refractive index at a wavelength of 10 μm is 2.276. The theoretical transmittance was then calculated using Equations (1) and (2) with ß = 0 and nm = 2.276. The resulting value of 72% [T% =(1-R)2 × 100 = 72%] indicated that it is possible to obtain a high transmittance almost in line with theoretical values.

Table 2 shows other characteristics. The material retains practical strength, but Knoop hardness is a low 370 compared to Ge (800), so machinability is outstanding, and it can easily be shaped into an aspherical lens.

3-2 High-Temperature Characteristics

Figure 17 shows the temperature dependence of in-line transmittance in the infrared range for a 3 mm thick sample. At wavelengths of 10 μm and below, temperature has little effect, and the material exhibits almost stable translucence. However, in the long wavelength range of 10 μm and above, the infrared absorption edge is shifted toward shorter wavelengths, and there is an evident tendency for the translucence range to narrow. This infrared absorption edge is determined, in principle, by the multi-phonon mode lattice vibration peculiar to each material. As temperature increases, the internal energy of the substance increases and the lattice vibration frequency shifts in the high-energy direction, so there is a shift in absorption toward short wavelengths. Consequently if high temperature use is anticipated, the effects of the temperature on transmittance must be given careful attention.

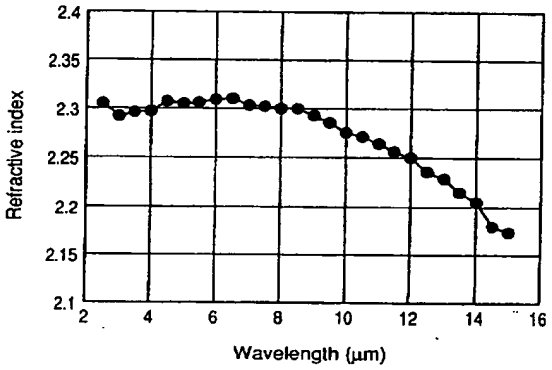

Fig. 16. Refractive index of a ZnS sintered body

Table 2. Typical characteristics of a ZnS sintered body

Term	Unit	ZnS sintered body
Melting point	K	2103
Density	$\times 10^3$ kg/m^3	4.09
Refractive index at 10 μm		2.28
Young's modulus	GPa	75
Flexural strength	MPa	93
Knoop hardness number		370
Thermal conductivity	W/(m · K)	19.1
Thermal expansion coefficient 20 ~ 300°C	$\times 10^{-6}$/K	6.7

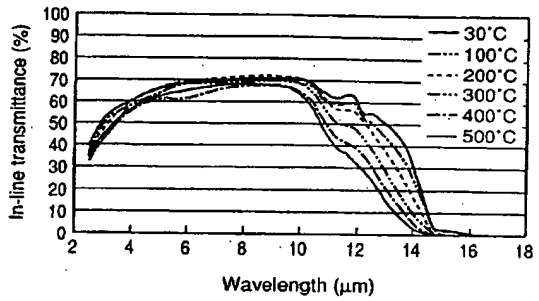

Fig. 17. Transmittance of a ZnS sintered body, at elevated temperatures

3-3 Strength Analysis

For this ZnS sintered body to be incorporated into systems as an optical component, the reliability of the structural design in terms of strength is crucial. We therefore conducted analysis using Weibull statistics, which are used to evaluate the strength of brittle materials.

As the subject for evaluation, we fabricated panel material of dimensions ø100 × 10 mm, freely cut out bending test pieces from that, and measured the strength distribution. For this test the 4-point bending method based on JISR1601 was employed using n = 20, and the probability of failure of each data was allocated based on the mediarank method. The results are shown in **Figure 18**. Analysis of results using the least square method indicated a Weibull coefficient of 6.1 and an average strength of 93 MPa. The stress with a probability

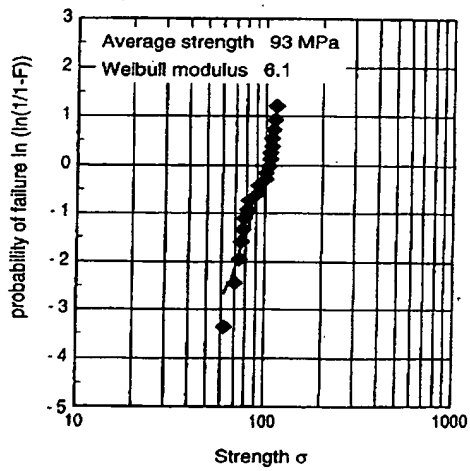

Fig. 18. Weibull distribution analysis of a ZnS sintered body

of failure of 0.1% is 47 MPa, and the stress with a probability of failure of 0.01% is 32 MPa.

Using these results it is now possible to perform strength design for actual products, based on the effective volume inferred from the product form and usage conditions.

3-4 Product Form

Using this technology it has been found possible to fabricate product forms from small units of ø10 mm or less up to large types of ø150 × 60 mm, and various applications such as for lenses and window materials are being studied.

4. Development of a ZnS sintered Body with Optic Filter Functionality

When detecting the human body using an infrared sensor, light not to be detected (in particular light in the visible to near/mid infrared range) becomes noise and may result in misoperation or a drop in detection precision. To help alleviate this, it was speculated that to achieve filter functionality the powder method could be further exploited by adding an element that has little absorption in the 8 to 12 μm wavelength range (area of required sensor sensitivity) but high absorption in the 0.4 to 3 μm wavelength visible to near/mid infrared range (area of noise). The details are described below.

4-1 Optical Design

To select possible elements to add, we first predicted the absorption wavelength by calculation. Light absorption by an added element occurs because light with the energy difference between the ground state and excited state is absorbed when the element's outer shell electrons are excited. Hence we calculated the energy of the ground state and excited state for each element, and then calculated the absorption wavelength (λ_{abs}) based on Equations (8) and (9) below.

$$\Delta E = E_{ex} - E_0 \quad \cdots\cdots (8)$$

Where:
E_{ex} : Energy of excited state
E_0 : Energy of ground state

$$\lambda_{abs} = hc/\Delta E \quad \cdots\cdots (9)$$

h : Planck's constant
c : Speed of light

We selected elements A, B, C and D from the possible candidates, having low absorption in the 8 to 12 μm wavelength range and high absorption in the 0.4 to 3 μm wavelength range. These were added based on the process in **Figure 19** to fabricate prototype sintered bodies. In-line transmittance in the visible to infrared range (wavelengths 0.4 to 15 μm) was measured for each of the fabricated sintered bodies, and it was found that

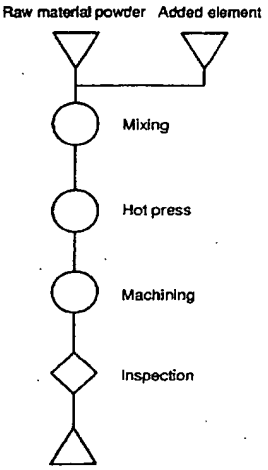

Fig. 19. Manufacturing process for a ZnS sintered body of optical filtering grade

there was no single element that could absorb the entire width of the noise wavelength range.

It was then decided to attempt to achieve light absorption over a wide range of wavelengths by using a combination of added elements.

As described above, the transmittance of infrared optical ceramics is given by the Lambert-Beer Equation (1), and if the material and thickness are specified, then the transmittance is determined by the absorption coefficient β. As indicated by Equation (3), the factor ß is comprised of the material specific absorption and other terms for scattering. However, if we assume here that the contribution of each element acts in a linear manner, β can be expressed as in Equation (10) using the absorption coefficients for each material.

$$\beta = \alpha_0 + S + \Sigma\alpha_i \cdot C_i \quad \cdots\cdots (10)$$

Where:
α_0 : Absorption coefficient distinctive to the material
S : Contribution to scattering
α_i : Absorption coefficient of added element i
C_i : Relative concentration of added element i

In order to first determine the absorption coefficients α_A to α_D of each element for the wavelengths 0.4 to 12 μm, we measured the in-line transmittance of sintered bodies to which each element had been added individually. Using Equations (1) and (10), an equation to determine the transmittance of a system in which each element has been added individually can be derived as in (11).

$$Ti = (1-R)^2 \cdot \exp\{-\underbrace{(\alpha_0 + S + \alpha_i \cdot C_i)}_{\beta_i}\, t\} \quad \cdots\cdots (11)$$

Where:
Ti : transmittance of a system to which element i has been added

From Equation (1), α_0 and S are determined by the transmittance T_0, reflectance R and sample thickness t

of the ZnS sintered body to which nothing has been added. Hence the absorption coefficient α_i of the added element can be obtained using the measured transmittance Ti and the known added concentration C_i. The absorption coefficients obtained for each element A to D are shown in **Figure 20**. As can be seen, each element has distinctive absorption in each wavelength range.

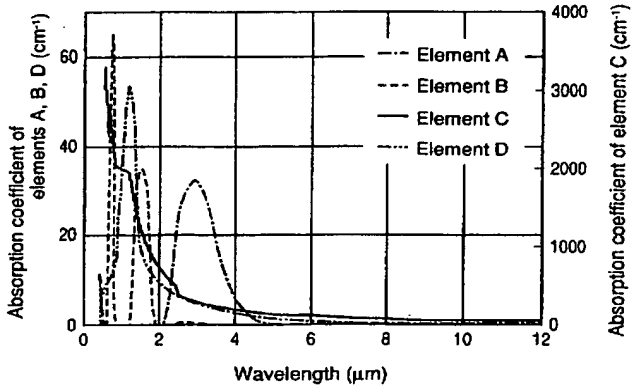

Fig. 20. Absorption coefficients of additive elements

4-2 Combined Addition

Using the absorption coefficients of each element found in the previous section, we selected additive elements to enable absorption of a wide range of light with wavelengths from 0.4 to 3 μm, and thereby performed combined additive design. Based on this design, materials were prototyped using the process in **Fig. 19**, and the results are shown in **Figure 21**.

Combined additive type 1 uses A, B and C as the additive elements, and combined additive type 2 used A, B and D. With both types, the designed calculated values agreed well with actual measurements.

These results confirmed that this design technique is effective, and that it is possible to freely design filters using different types and added amounts of the additive elements.

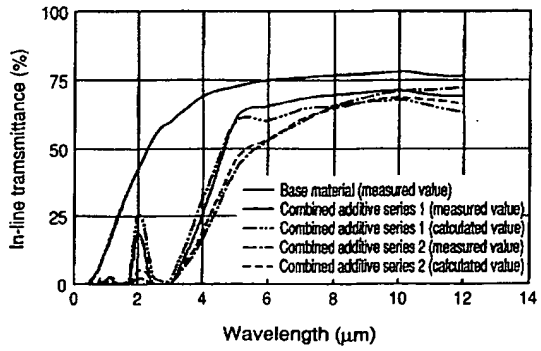

Fig. 21. Comparison of transmittance between calculated and measured values of ZnS sintered bodies of optical filtering grade

5. Conclusions

An infrared translucent ZnS sintered body manufacturing process has been established that uses a powder sintering method and shows excellent potential for economic mass production.

Through precise control of residual pore diameter using pressurized sintering technology, the sintered bodies have performance equivalent to that of CVD-ZnS in the wavelength ranges of 8 to 12 μm and 3 to 5 μm.

In a further development, a ZnS sintered body has been produced with light filtering functionality that cuts problematic visible to near/mid infrared noise, achieved by adding mixtures of elements.

Applications for this technology include human body detection, an area of use that is expected to grow steadily in the future.

Reference

(1) Paul: Klocek: Handbook of infrared optical materials, Marcel Dekker inc (1991)
(2) Doi and others : SEI Technical Review No.124, p.94 (1984)
(3) Fujii et al.,: SEI Technical Review No.154, p.96 (1999)
(4) Fujii et al.,: SEI Technical Review No.155, p.120 (1999)
(5) Katsumi Miyauchi and others: Opto Ceramics, Gihodo publication (1984)
(6) H. C. van deHulst : Light Scattering by Small Particles, John Wiley and Sone, Inc., New New York (1957)

Contributors

M. HASEGAWA
- Structural Components and Materials R&D Department, Itami R&D Laboratories

O. KOMURA
- Chief Research Associate, Structural Components and Materials R&D Department, Itami R&D Laboratories

A. YAMAKAWA
- Dr.Eng., Manager, Structural Components and Materials R&D Department, Itami R&D Laboratories

K. SHIBATA
- Senior Assistant Manager, Hybrid Products Division

H. NAITO
- Assistant Manager, Hybrid Products Division, Engeneering Department

S. NAKAYAMA
- Assistant Manager, Hybrid Products Division, Engeneering Department

A. FUJII
- Senior Staff, Hybrid Products Division, Engeneering Department

SUMITOMO ELECTRIC INDUSTRIES, LTD.

Head Office (Osaka) 5-33, Kitahama 4-chome, Chuo-ku, Osaka, 541-0041 Japan
TEL: (06) 6220-4141 FAX: (06) 6222-3380 URL: http://www.sei.co.jp/

Head Office (Tokyo) 3-12, Moto-Akasaka 1-chome, Minato-ku, Tokyo, 107-8468 Japan
TEL: (03) 3423-5111 FAX: (03) 3423-5009

Overseas Offices

Sumitomo Electric U.S.A., Inc. (New York Head Office)
One North Lexington Avenue, 16th Floor, White Plains, N.Y. 10601, U.S.A.
TEL: (914) 467-6001 FAX: (914) 467-6081

Sumitomo Electric U.S.A., Inc. (Los Angeles Branch Office) 21221 S.Western Avenue, Suite 200, Torrance
CA. 90501, U.S.A. TEL: (310) 782-0227 FAX: (310) 782-0211

Sumitomo Electric Europe Ltd. Unit220 Centennial Avenue, Centennial Park, Elstree Hill South, Elstree,
Hartfordshire WD6 3SL, England, United Kingdom
TEL: (208) 953-8118 FAX: (208) 207-5950

Sumitomo Electric Asia, Ltd. Room 3408, Windsor House, 311 Gloucester Road, Causeway Bay, Hong Kong
TEL: (25) 76-0080 FAX: (25) 76-6412

Sumitomo Electric International (Singapore) Pte., Ltd. 100 Beach Road, Shaw Towers, #24-07 Singapore 189702
TEL: (291) 7525 FAX: (291) 7502

Attached Document

	Ceramic raw material from Table 2				Resin raw material from Table 4				Correction calculation								Calculated value	Lens from Table 5
	Ceramic	Transmittance		Ti/Tv(ceramic)	Resin	Thickness	Transmittance		Refractive index	Absorption coefficient	Refractive index	Absorption coefficient	Corrected thickness	Corrected transmittance		After correction	Ti/Tv(ceramic) × Ti/Tv(resin)	Ti/Tv(lens)
		Ti	Tv			t	Ti	Tv	ni	βi	nv	βv	t	Ti	Tv	Ti/Tv(resin)		
1	2	52.1	0.016	3170	1	0.1	81	74	1.6	1.012712	1.5	2.195	0.02	87.8	88.2	1.0	3157	4177
2	2	52.1	0.016	3170	1	0.1	81	74	1.6	1.012712	1.5	2.195	0.03	87.0	86.3	1.0	3194	4247
3	2	52.1	0.016	3170	1	0.1	81	74	1.6	1.012712	1.5	2.195	0.05	85.2	82.6	1.0	3271	4474
4	2	52.1	0.016	3170	1	0.1	81	74	1.6	1.012712	1.5	2.195	0.1	81.0	74.0	1.1	3470	5015
5	2	52.1	0.016	3170	1	0.1	81	74	1.6	1.012712	1.5	2.195	0.11	80.2	72.4	1.1	3511	5130
6	2	52.1	0.016	3170	2	0.1	40	11	1.6	8.068409	1.5	21.256	0.05	59.9	31.8	1.9	5961	9889
7	2	52.1	0.016	3170	12	0.1	57	48	1.6	4.526691	1.5	6.523	0.05	71.5	66.5	1.1	3407	19438
8	12	26.1	1.15E-05	2270000	1	0.1	81	74	1.6	1.012712	1.5	2.195	0.05	85.2	82.6	1.0	2342149	3680000
9	12	26.1	1.15E-05	2270000	2	0.1	40	11	1.6	8.068409	1.5	21.256	0.05	59.9	31.8	1.9	4268955	7080000
10	12	26.1	1.15E-05	2270000	12	0.1	57	48	1.6	4.526691	1.5	6.523	0.05	71.5	66.5	1.1	2439522	12800000
11	18	70.8	12.1	5.9	2	0.1	40	11	1.6	8.068409	1.5	21.256	0.05	59.9	31.8	1.9	11	18.3
12	18	70.8	12.1	5.9	12	0.1	57	48	1.6	4.526691	1.5	6.523	0.05	71.5	66.5	1.1	6	33.1
13	19	53	0.095	556	12	0.1	57	48	1.6	4.526691	1.5	6.523	0.05	71.5	66.5	1.1	598	3138
14	21	61.9	0.15	406	1	0.1	81	74	1.6	1.012712	1.5	2.195	0.05	85.2	82.6	1.0	419	576
15	21	61.9	0.15	406	2	0.1	40	11	1.6	8.068409	1.5	21.256	0.05	59.9	31.8	1.9	764	1066
16	21	61.9	0.15	406	12	0.1	57	48	1.6	4.526691	1.5	6.523	0.05	71.5	66.5	1.1	436	2033
17	28	71.3	13.5	5.3	1	0.1	81	74	1.6	1.012712	1.5	2.195	0.05	85.2	82.6	1.0	5	7.5
18	28	71.3	13.5	5.3	2	0.1	40	11	1.6	8.068409	1.5	21.256	0.05	59.9	31.8	1.9	10	13.9
19	28	71.3	13.5	5.3	12	0.1	57	48	1.6	4.526691	1.5	6.523	0.05	71.5	66.5	1.1	6	25.2
20	30	54.3	0.8	67.9	2	0.1	40	11	1.6	8.068409	1.5	21.256	0.05	59.9	31.8	1.9	128	176
21	30	54.3	0.8	67.9	12	0.1	57	48	1.6	4.526691	1.5	6.523	0.05	71.5	66.5	1.1	73	318
				(*1)												(*2)	(*1 × *2)	

Note: Samples indicated by the Examiner are No. 3 and No. 6. In this table, all samples have corrected results smaller than Ti/Tv(lens) of Table 5.